

Dwarf Novae in the Shortest Orbital Period Regime: I. A New Short Period Dwarf Nova, OT J055717+683226

Makoto UEMURA¹, Akira ARAI², Taichi KATO³, Hiroyuki MAEHARA⁴,
Daisaku NOGAMI⁵, Kaori KUBOTA³, Yuuki MORITANI³, Akira IMADA⁶,
Toshihiro OMODAKA⁶, Shota OIZUMI⁶, Takashi OHSUGI¹,
Takuya YAMASHITA⁷, Koji S. KAWABATA¹, Mizuki ISOGAI²,
Osamu NAGAE⁸, Mahito SASADA⁸, Hisashi MIYAMOTO⁸, Takeshi UEHARA⁸,
Hiroyuki TANAKA⁸, Risako MATSUI⁸, Yasushi FUKAZAWA⁸, Shuji SATO⁹,
and Masaru KINO⁹

¹*Astrophysical Science Center, Hiroshima University, Kagamiyama 1-3-1,
Higashi-Hiroshima 739-8526
uemuram@hiroshima-u.ac.jp*

²*Department of Physics, Faculty of Science, Kyoto Sangyo University,
Motoyama, Kamigamo, Kita-ku, Kyoto 603-8555*

³*Department of Astronomy, Faculty of Science, Kyoto University, Sakyo-ku, Kyoto 606-8502*

⁴*Kwasan Observatory, Kyoto University, Ohmine-cho Kita Kazan, Yamashina-ku, Kyoto, 607-8471*

⁵*Hida Observatory, Kyoto University, Kamitakara, Gifu 506-1314*

⁶*Faculty of Science, Kagoshima University, 1-21-30, Korimoto, Kagoshima 890-0065*

⁷*National Astronomical Observatory of Japan, 2-21-1 Osawa, Mitaka, Tokyo 181-8588*

⁸*Department of Physical Science, Hiroshima University, Kagamiyama 1-3-1,
Higashi-Hiroshima 739-8526*

⁹*Department of Physics, Nagoya University, Furo-cho, Chikusa-ku, Nagoya 464-8602*

(Received 2008 July 27; accepted 2009 December 22)

Abstract

We report the observation of a new dwarf nova, OT J055717+683226, during its first-ever recorded superoutburst in December 2006. Our observation shows that this object is an SU UMa-type dwarf nova having a very short superhump period of 76.67 ± 0.03 min (0.05324 ± 0.00002 d). The next superoutburst was observed in March 2008. The recurrence time of superoutbursts (supercycle) is, hence, estimated to be ~ 480 d. The supercycle is much shorter than those of WZ Sge-type dwarf novae having supercycles of $\gtrsim 10$ yr, which are a major population of dwarf novae in the shortest orbital period regime ($\lesssim 85$ min). Using a hierarchical cluster analysis, we identified seven groups of dwarf novae in the shortest orbital period regime. We identified a small group of objects that have short supercycles, small outburst amplitudes, and large superhump period excesses, compared with those of WZ Sge stars. OT J055717+683226 probably belongs to this group.

Key words: accretion, accretion disks—stars: novae, cataclysmic variables—stars: individual(OT J055717+683226)

1. Introduction

Dwarf novae (DNe) are a subclass of cataclysmic variable stars (CVs) and consist of a close binary system containing a white dwarf and a Roche-lobe filling red-dwarf star (Warner 1995a). The orbital periods (P_{orb}) of ordinary hydrogen-rich DNe range from 76 min to 5.7 d (Ritter, Kolb 2003). DNe having short orbital periods of $76 \text{ min} \lesssim P_{\text{orb}} \lesssim 3 \text{ hr}$ tend to exhibit two types of outbursts, normal outbursts and superoutbursts. Such systems are called SU UMa-type DNe. SU UMa stars exhibit short-term periodic modulations, so-called superhumps, during superoutbursts. Superhumps can be a good indicator of the orbital period of a binary system because it is well known that their periods are slightly (about a few percent) longer than the orbital period (e.g. Warner 1995b). The

outburst behavior of SU UMa stars can be explained by the thermal–tidal instability model for the accretion disk around the white dwarf (for a review, see Osaki 1996).

It is widely believed that the evolution of a CV having $P_{\text{orb}} \lesssim 3 \text{ hr}$ is driven by angular momentum removal from the binary, associated with gravitational radiation (Paczynski 1981; Rappaport et al. 1982). By losing angular momentum, the CV evolves toward a shorter P_{orb} regime, until the onset of degeneracy in the secondary star. After the onset of degeneracy, the CV evolves toward a longer P_{orb} regime since the mass–radius relation of the secondary star changes. This scenario gives a qualitative explanation for the presence of a short-period cut-off at $P_{\text{orb}} \sim 76 \text{ min}$ in the observed P_{orb} distribution. However, the predicted period minimum (P_{min}) is significantly shorter than the observed minimum (Kolb 1993;

Kolb, Baraffe 1999; Renvoizé et al. 2002).

There are two notable exceptions of hydrogen-rich CVs having P_{orb} much shorter than the well-known P_{min} at ~ 76 min: V485 Cen ($P_{\text{orb}} = 59.0$) and EI Psc ($P_{\text{orb}} = 64.2$). A characteristic feature of these two is clear TiO absorption bands observed in their quiescent spectrum, which indicate luminous secondary stars. It is proposed that these systems have evolved secondaries and as a result their evolutionary paths are different from that of CVs having a main-sequence secondary (Augusteijn et al. 1996; Thorstensen et al. 2002a). Uemura et al. (2002) proposed that V485 Cen-like objects may be progenitors of helium CVs, so-called AM CVn stars, which are recognized as being interacting double white dwarfs. If this is the case, we can expect that progenitors of V485 Cen-like objects are hidden in the CV population having $P_{\text{orb}} > 76$ min. Such objects should have evolved secondaries, and hence, high mass-transfer rates compared with CVs having main-sequence secondaries (Podsiadlowski et al. 2003).

Thorstensen et al. (2002b) pointed out that there is a large diversity in DNe having very short P_{orb} , particularly in terms of the recurrence time of superoutbursts (super-cycle; T_s). It is well known that most systems have quite long supercycles of $T_s \gtrsim 10$ yr in the shortest period regime of $76 \text{ min} \lesssim P_{\text{orb}} \lesssim 85 \text{ min}$. These are called WZ Sge stars (Kato et al. 2001b). The shortest P_{orb} regime also includes ER UMa stars, such as DI UMa ($P_{\text{orb}} = 78.5722$ min), which have very short T_s (20–50 d) (e.g. Kato, Kunjaya 1995; Ishioka et al. 2001a). V844 Her is a unique object also having quite short P_{orb} (78.6859 min) in terms of the intermediate T_s (260 d), which is rather typical for a DN having a longer period of $P_{\text{orb}} \gtrsim 90$ min (Kato et al. 2003a; Kato, Uemura 2000). The nature of the diversity in T_s is poorly understood.

According to the disk instability model, T_s depends on the mass-transfer rate; a higher mass-transfer rate yields a short T_s (Osaki 1995b). The mass-transfer rate at each P_{orb} depends on the binary parameters, such as the structure of the secondary star. Hence, the diversity in T_s possibly indicates that DNe in the shortest P_{orb} regime includes several groups with different secondary star structures, or in other words different evolutionary paths of the binary. Alternatively, it is possible that the diversity in T_s arises from the diversity of the disk structure or the outburst mechanism. In order to investigate the origin of the T_s diversity, detailed studies are required of the sub-groups which may be present in the shortest P_{orb} regime, though the number of objects is small, apart from WZ Sge stars.

In this paper we report detailed observations of a new DN having a short P_{orb} . The object, OT J055717+683226 (hereafter, J0557+68), was discovered on an image taken on 2006 Dec 16.6 (UT) by W. Kloehr (Kloehr et al. 2006). Our time-series observations showed periodic modulations analogous to superhumps observed in SU UMa-type DNe (Uemura, Arai 2006). We also found that J0557+68 is a peculiar system in terms of its T_s , which is much shorter than those of WZ Sge stars.

As well as J0557+68, several objects in the shortest P_{orb}

regime have recently been discovered and well studied. The increasing sample size of short- P_{orb} DNe now allows us to perform a quantitative classification of DNe.

In the next section, we describe our observation equipment and image reduction. In § 3, we report the detailed outburst features of J0557+68. In § 4, we provide a new exploratory classification of DNe using a hierarchical cluster analysis. We also discuss the nature of J0557+68 and the origin of the diversity in T_s in the shortest P_{orb} regime. In the final section, we summarize our findings.

2. Observations

We performed optical and infrared observations of J0557+68 using TRISPEC, attached to the “KANATA” 1.5-m telescope at Higashi-Hiroshima Observatory. TRISPEC is a simultaneous imager and spectrograph with polarimetry covering both optical and near-infrared wavelengths (Watanabe et al. 2005). We used the imaging mode of TRISPEC with V , J , and K_s filters. The effective exposure times for each frame were 63, 60, and 54 s in the V , J , and K_s bands, respectively. After making dark-subtracted and flat-fielded images, we measured the V magnitudes of J0557+68 using a comparison star located at R.A. = $05^{\text{h}}57^{\text{m}}29^{\text{s}}105$, Dec. = $+68^{\circ}29'18''.88$ ($V = 13.39$). The J and K_s magnitudes were measured using a comparison star at R.A. = $05^{\text{h}}57^{\text{m}}39^{\text{s}}60$, Dec. = $+68^{\circ}33'34''.2$ ($J = 12.255$ and $K_s = 11.937$). We took the V magnitude of the comparison stars from the HIPPARCOS and TYCHO catalogues (Perryman, ESA 1997) and the J and K_s magnitudes from the 2MASS catalog (Skrutskie et al. 2006). We checked the constancy of the comparison stars using neighboring stars and found that they exhibited no significant variations over 0.01, 0.02, and 0.05 mag in the V , J , and K_s bands, respectively. Unfortunately, we could only obtain J -band images on JD 2454088 and 2454089 during the first outburst due to a failure of a filter wheel in the instrument. Heliocentric corrections were performed for each data set used for period analysis.

We show example optical CCD images in figure 1. J0557+68 is marked with the black bars. The image in the left panel was taken on JD 2454088, during the outburst. The right image was taken on JD 2454411, about 11 months after the outburst when the object was at quiescence.

We also performed optical photometric observations with other small telescope during the period of JD 2454087–2454114. The magnitudes with a clear filter and without any filters were adjusted to the V -band system of TRISPEC/KANATA by adding constants.¹ Table 1 details our observation log and instruments at each observatory.

Using neighboring USNO B1.0 stars, we calculated the position of J0557+68 from 10 V -band images on JD 2454088 obtained with TRISPEC/KANATA. The

¹ The clear filter is made of the optical glass in a thickness comparable to other filters. The total efficiency with the clear filter is slightly different from that without filters since the clear filter has its own transmission curve.

Table 1. Observation log and our equipment.

Site	Telescope	Camera	Filter	Date (+JD2454000)
Higashi-Hiroshima Astr. Obs.	1.5-m	TRISPEC	V, J, K_s	88, 89, 91, 92, 96, 97, 100, 105, 114, 123, 125, 126, 127, 130, 131, 148, 151, 152, 153, 155, 412, 543, 547
Saitama	25-cm	SBIG ST-7XME	clear	87, 89, 92, 93, 97, 99, 543, 547
Kyoto Univ.	40-cm	SBIG ST-9	none	101, 105, 109, 110, 111, 112, 113, 114
Kagoshima Univ.	1.0-m		none	101

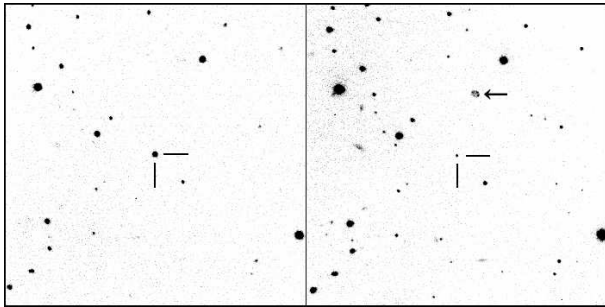


Fig. 1. V -band images of J0557+68 in outburst (left panel) and in quiescence (right panel) observed with the KANATA 1.5-m telescope. The field of view is $5' \times 5'$; north is up and east is to the left. The two black bars indicate J0557+68. The diffuse source indicated by the arrow in the right panel is a ghost image.

average position is R.A. = $05^{\text{h}}57^{\text{m}}18^{\text{s}}.487$, Dec. = $+68^{\circ}32'27''.01$ with a systematic error of $0''.18$. Within the error of the position, a faint USNO B1.0 star with $b = 19.04$ and $r = 19.23$ could be observed, which is considered to be the quiescent counterpart of J0557+68. A ROSAT X-ray source at $25''$ apart from J0557+68 could also be observed, which is probably the X-ray counterpart.

3. Short-Period DN, J0557+68

3.1. Overall behavior of the 2006 and 2008 outbursts

The upper panel of figure 2 shows the light curve of an outburst of J0557+68 in 2006. The outburst continued for 14 days from its discovery (JD 2454085.6; Kloehr et al. 2006), with an average fading rate of $0.10 \pm 0.01 \text{ mag d}^{-1}$. These features are quite typical for superoutbursts in SU UMa-type DNe (Warner 1995b). This plateau phase was terminated by a rapid fading starting on JD 2454100. The object experienced a short rebrightening on JD 2454109. The duration of the rebrightening was ~ 5 days. Such single short rebrightening is occasionally observed in short period SU UMa stars (e.g. Baba et al. 2000; Imada et al. 2006a) and WZ Sge stars (e.g. Ishioka et al. 2001b; Templeton et al. 2006). After the rebrightening, the object again started a gradual fading. The object had almost returned to the quiescent state by JD 2454120. Our observation at quiescence (JD 2454412) yielded $V = 18.89 \pm 0.04$. The observed amplitude of the outburst is $\sim 4 \text{ mag}$. We note that this is the lower-limit of the amplitude since we possibly overlooked the early

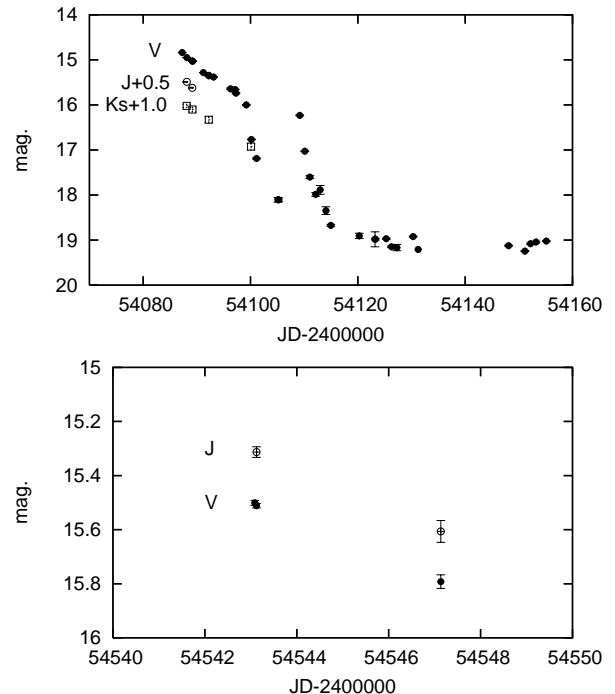


Fig. 2. Light curves of an outburst of J0557+68 in 2006 (upper panel) and 2008 (lower panel). The abscissa and ordinate denote the time in JD and the magnitude, respectively. The filled circles are V -band and unfiltered CCD observations. The open circles and squares are J and K_s -band observations, respectively. In the upper panel, the J and K_s magnitudes are shifted by $+0.5$ and $+1.0 \text{ mag}$, as indicated in the figure.

phase of the outburst.

We obtained simultaneous photometric data in the V and J -bands for two nights and in the V and K_s -bands for four nights. These near-infrared data are shown in figure 2. Using these multicolor data, we show temporal color variations in figure 3. As shown in figure 3, both the colors remained ~ 0 during the plateau phase, which is typical for DNe in outburst. In the rapid fading stage, a clear reddening of the object was observed in $V - K_s$.

The next outburst was observed in March 2008. We show the light curve of the 2008 outburst in the lower panel of figure 2. The object remained in a bright state for at least 4 days. The object was apparently fading at a rate of 0.07 mag d^{-1} during the outburst. These characteristics indicate that the 2008 outburst is another superoutburst. The time interval between the two superoutbursts is about

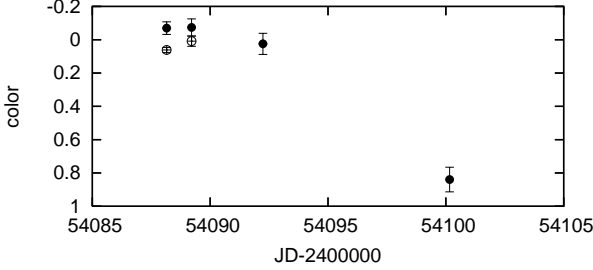


Fig. 3. Temporal evolution of colors. The abscissa and ordinate denote JD and the colors of $V - J$ and $V - K_s$. The open and filled circles are $V - J$ and $V - K_s$, respectively.

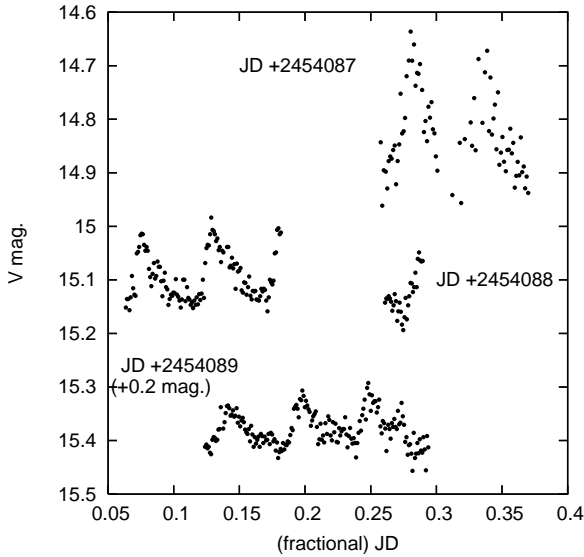


Fig. 4. Example superhumps observed in J0557+68. The abscissa denotes the time in JD, in which integer parts are subtracted. The ordinate denotes the V -magnitude. Light curves on JD 2454087, 2454088, and 2454089 are shown. The light curve on JD 2454089 is shifted by +0.2 mag.

480 d. We consider this to be a T_s of J0557+68, which is much shorter than those of WZ Sge stars (~ 10 yr) and rather comparable to those of normal SU UMa stars.

3.2. Superhumps

During the 2006 outburst, we detected short-term periodic modulations. Examples are shown in figure 4. The modulations had saw-tooth profiles with decreasing amplitude with time. These features are typical characteristics for superhumps (Uemura, Arai 2006). Together with the features of the whole light curve, the detection of the superhumps established that J0557+68 is an SU UMa-type DN and the 2006 outburst was a superoutburst.

We performed a period analysis for the superhumps using the phase dispersion minimization (PDM) method (Stellingwerf 1978). Before the PDM analysis, a linear fading trend was subtracted from the light curves during the superoutburst (JD 2454087–2454100). The light curves obtained with small telescopes have larger disper-

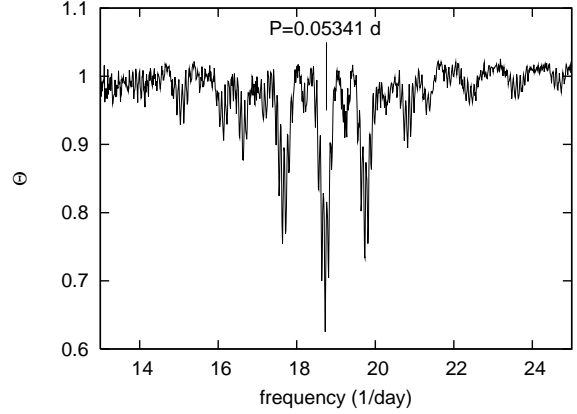


Fig. 5. Frequency– Θ diagram defined by the PDM method (Stellingwerf 1978). The best candidate of the frequency is marked in the figure.

sions than those obtained with the KANATA telescope. By binning these light curves into neighboring three-point bins, we obtained data with similar dispersions. We excluded observations on JD 2454092 and 2454093 from the sample for our period analysis since the phase of modulations changed on these nights, as mentioned below. As a result, we obtained 620 photometric points. Using these data, we calculated Θ defined in the PDM method for each frequency. The frequency– Θ diagram is shown in figure 5. A strong signal can be seen at ~ 0.05341 d.

Figure 6 presents the temporal evolution of the superhump profiles. Short-term modulations observed after the superoutburst are also included in this figure. The light curves were folded by a period of 0.05341 d. As mentioned above, the superhump decreased in amplitude during the early phase of the superoutburst, as can be seen in figure 6 (labeled as “JD2454087”, “88”, “89”, and “91”). As the main hump weakened, the secondary hump appears to become prominent. As a result, the hump had a double-peaked profile with the phase apparently inverted in several humps (“92”, “93”, “97”). Just before and after the rapid fading stage, the hump profiles became complicated, while hints of superhumps and their secondary humps can be seen (“99”, “100”, “101”). During the rebrightening, clear humps were observed, while their phase was shifted compared with the superhumps. They had sinusoidal profiles rather than the typical saw-tooth profiles (“109”, “110”).

To explore the temporal variation of the superhump period, we calculated $O - C$ of the superhumps. The detailed procedure to determine the peak times of the superhumps is shown in Kato et al. (2009). We calculated $O - C$ for them with a period of 0.05341 d and the epoch of HJD 2454087.2836, the first superhump maximum we observed. The $O - C$ and the time of the superhump maxima are listed in table 2. The $O - C$ diagram is depicted in figure 7. In the table and figure, E denotes the cycle number of the superhumps. As described above, the phase of the prominent hump was inverted in the cycles 91, 92, and 94. $O - C$ for these secondary humps are also listed

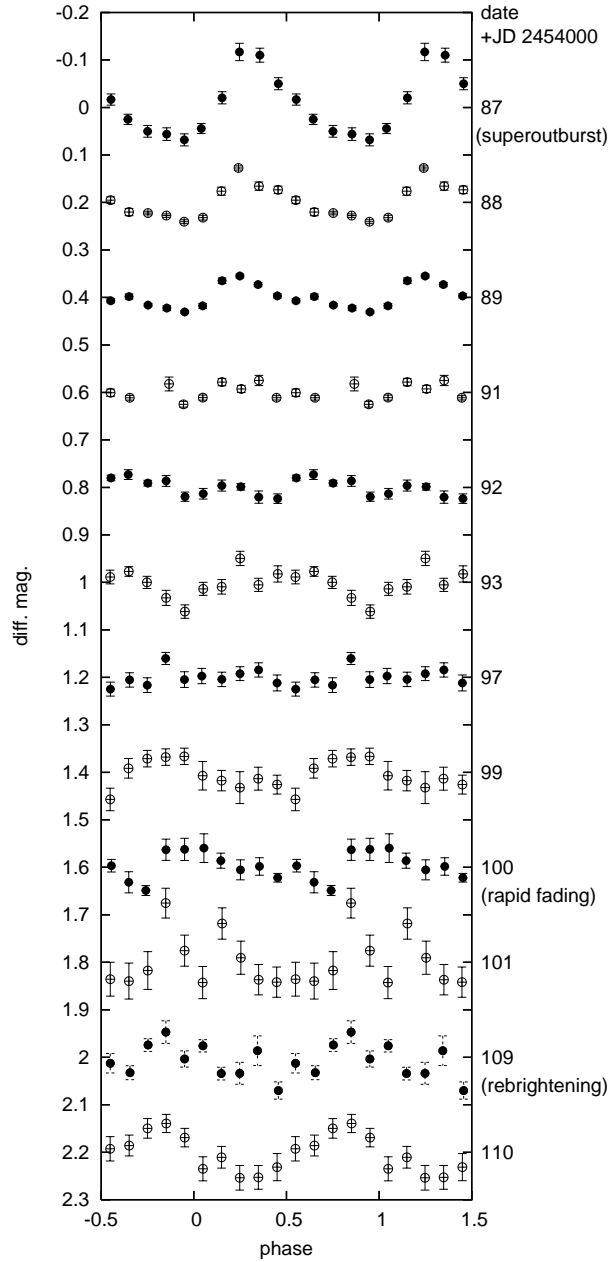


Fig. 6. Phase-averaged light curves of superhumps. The abscissa and ordinate denote the superhump phase and the differential magnitude, respectively. The superhump phase was defined by an arbitrary epoch and the superhump period of 0.05341 d. Temporal variations of the superhump profile are shown from JD 2454087 (top) to JD 2454110 (bottom). Each light curve is shifted by 0.2 mag.

Table 2. $O - C$ of superhumps.

E	$O - C$ (d)	Error (d)	Superhump peak (HJD-2400000)
0	-0.0004	0.0007	54087.2836
1	-0.0009	0.0011	54087.3365
15	-0.0020	0.0005	54088.0832
16	-0.0013	0.0006	54088.1373
17	-0.0053	0.0012	54088.1868
19	-0.0013	0.0006	54088.2976
20	-0.0036	0.0005	54088.3487
34	-0.0030	0.0009	54089.0971
35	-0.0057	0.0009	54089.1479
36	-0.0051	0.0010	54089.2018
37	-0.0043	0.0010	54089.2561
38	-0.0054	0.0008	54089.3084
39	-0.0050	0.0008	54089.3622
49	-0.0047	0.0019	54089.8967
50	0.0007	0.0012	54089.9555
51	-0.0027	0.0011	54090.0055
52	-0.0041	0.0042	54090.0575
54	-0.0014	0.0031	54090.1670
74	0.0020	0.0019	54091.2387
91	-0.0030	0.0082	54092.1346
92	-0.0068	0.0083	54092.1842
94	-0.0021	0.0084	54092.2955
(91)	-0.0343	0.0022	54092.1621
(92)	-0.0317	0.0019	54092.2180
(93)	-0.0333	0.0019	54092.2697
(94)	-0.0341	0.0022	54092.3222
109	0.0085	0.0048	54093.1147
110	0.0112	0.0051	54093.1708
143	0.0041	0.0021	54094.9264
144	0.0050	0.0026	54094.9808
180	-0.0003	0.0044	54096.8984
183	-0.0002	0.0062	54097.0587
185	-0.0216	0.0073	54097.1442
257	-0.0157	0.0024	54100.9959
258	-0.0014	0.0040	54101.0637
259	-0.0122	0.0025	54101.1063
260	-0.0242	0.0021	54101.1477

in the table and figure.

Figure 7 show a possible period change of superhumps. Koen (2006) provides a method to test the significance of a period change seen in $O - C$ diagrams. We applied this method to the $O - C$ of J0557+68. Koen (2006) considers two mechanisms which cause $O - C$ variations, a random cycle-to-cycle jitter and a real period variation. Four models for $O - C$ variations are then introduced: neither cycle-to-cycle jitter nor period change (Model 1), a significant cycle-to-cycle jitter and no period change (Model 2), a significant period change and no cycle-to-cycle jitter (Model 3), and both a significant cycle-to-cycle jitter and a period change (Model 4). The goodness of fit of the models is evaluated with two information criteria (IC), the Akaike and Bayes IC (AIC and BIC). Probabilities for the models are finally calculated with each IC. We

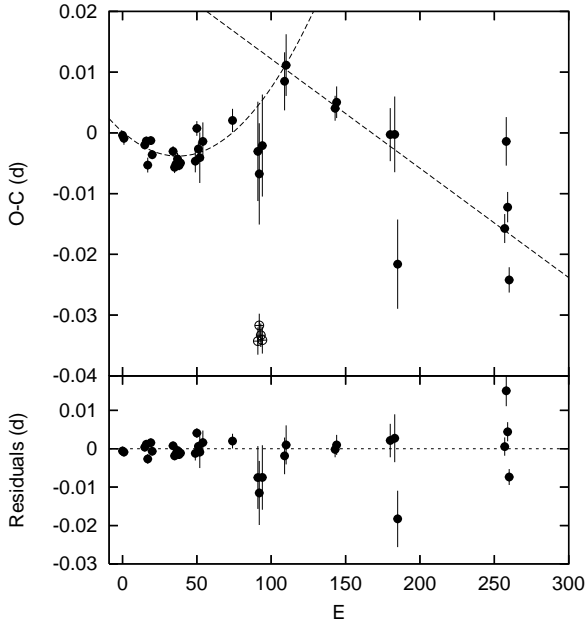


Fig. 7. $O - C$ diagram of superhumps in J0557+68. The abscissa and ordinate denote the cycle number of superhumps and $O - C$ in days, respectively. The dashed lines are the best-fit lines for $O - C$ in the early and late stages (for detail, see the text). The open circles indicate the secondary humps prominent in cycles 91, 92, and 94.

Table 3. Probabilities for the models in Koen (2006).

Model*	P_a^\dagger	P_b^\ddagger
Early phase ($0 \leq E \leq 74$)		
M1	0.02	0.02
M2	0.20	0.20
M3	0.64	0.63
M4	0.14	0.15
Late phase ($109 \leq E$)		
M1	0.59	0.41
M2	0.22	0.28
M3	0.17	0.22
M4	0.02	0.09

* For description of the models, see the text.

† Probability calculated from Akaike information criterion.

‡ Probability calculated from Bayesian information criterion.

calculated the probabilities using the $O - C$ observed in J0557+68 in an early phase of $0 \leq E \leq 74$ and a late phase of $109 \leq E$. The results are listed in table 3. In this table, P_a and P_b denote the probabilities calculated from AIC and BIC, respectively. Model 3 and Model 1 have the highest probabilities among the four models in the early and late phases, respectively.

The result of the Koen's test indicates that P_{SH} of J0557+68 changed with time in an early phase, and then became constant in a late phase of the superoutburst. The

Table 4. Best-fit parameters for the $O - C$ model of J0557+68.

a	$2.87 \pm 0.56 \times 10^{-6}$
b	$-2.15 \pm 0.37 \times 10^{-5}$
c	$1.78 \pm 5.28 \times 10^{-4}$
T	108 ± 7
p	$-1.80 \pm 0.21 \times 10^{-5}$
q	$3.02 \pm 0.70 \times 10^{-2}$
P_{dot}	$10.8 \pm 2.2 \times 10^{-5}$
P_2^\dagger	0.05324 ± 0.00002

* Period derivative in the early phase.

† Period in the late phase.

transition occurred in $74 < E < 109$. Assuming a constant period derivative, these features can be modeled as follows:

$$(O - C)_{\text{early}}(E) = aE^2 + bE + c \quad (0 \leq E \leq T), \quad (1)$$

$$(O - C)_{\text{late}}(E) = pE + q \quad (E > T), \quad (2)$$

$$(O - C)_{\text{early}}(T) = (O - C)_{\text{late}}(T). \quad (3)$$

Equation (3) is needed in order to ensure the continuity of the $O - C$ variation. The best-fit parameters and their uncertainties were calculated with a Bayesian approach in which probability densities of the parameters were estimated using a Markov-Chain Monte Carlo (MCMC) algorithm (Metropolis 1953; Gilks et al. 1996). Table 4 lists the obtained best-fit parameters for the observed $O - C$ of J0557+68. We confirmed that the obtained T ($= 108 \pm 7$ d) is consistent with that expected from the Koen's test ($74 < E < 109$). The model with those best-fitted parameters is indicated by the dashed line in figure 7. The period derivative of the early phase ($P_{\text{dot}} = P_{\text{SH}}/P_{\text{SH}}$) and the period of the late phase (P_2) are also included in the table. The positive period derivative means a period increase of superhumps in the early phase.

According to Kato et al. (2009), SU UMa-type DNe generally has three stages in term of P_{SH} : stage A with a long P_{SH} , stage B with a positive period derivative, and stage C with a short P_{SH} . The $O - C$ variation of J0557+68 can be interpreted as a transition from stage B to C. The duration of stage A is so short (1–2 d) that it was probably missed in the case of J0557+68. Kato et al. (2009) suggested that the minimum P_{SH} , either P_2 or P_{SH} at the start of stage B, is regarded as a representative P_{SH} of an object. The representative P_{SH} of J0557+68 is, then, $P_2 = 0.05324 \pm 0.00002$ d.

To date, GW Lib has the shortest P_{orb} among ordinary hydrogen-rich CVs except for V485 Cen and EI Psc, that is, $P_{\text{orb}} = 0.05332 \pm 0.00002$ d (Thorstensen et al. 2002b). VS 0329+1250 possibly has a shorter P_{orb} since its superhump period is quite short ($P_{\text{SH}} = 0.053394 \pm 0.00007$ d; Shafter et al. 2007). As shown in table 4, J0557+68 is definitely one of SU UMa stars having the shortest P_{orb} . V485 Cen and EI Psc are hydrogen-rich DNe having atypically short P_{orb} (~ 60 min). However, they are considered to have an evolutionary path different from those of CVs

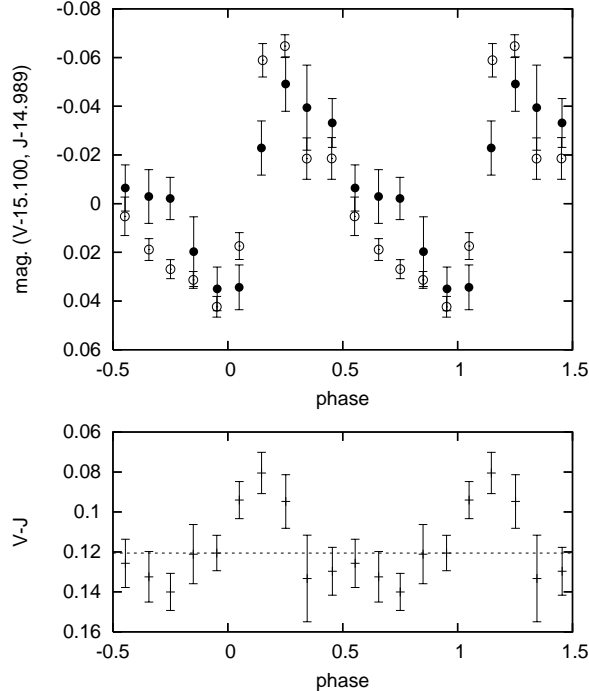


Fig. 8. Upper panel: Phase-averaged superhump profiles in the V and J -bands on JD 2454088. The abscissa and ordinate denote the superhump phase and magnitude, respectively. The open and filled circles are observations in the V and J -bands, respectively. Both the light curves are normalized to be readily compared. Lower panel: $V - J$ color variation associated with the superhump. The dashed line indicates the color at the bottom of the superhumps.

having main-sequence secondaries (for details, see § 1 and 4).

3.3. Simultaneous optical and near infrared observation of superhumps

We successfully performed simultaneous V and J -band time-series observations on JD 2454088. Superhumps were observed in both bands. The phase-averaged profiles and colors are shown in figure 8. In the rising phase of the superhump, the V -band flux brightened more rapidly than the J -band flux. As a result, the bluest phase preceded the superhump maximum. After the superhump maximum, the V -band flux decreased rapidly, while the decrease of the J -band flux was rather gradual. In addition, we can see a secondary hump at a phase of ~ 0.7 only in the J -band. The behavior in the J -band results in a rapid reddening, as can be seen in the lower panel of figure 8. The color during the secondary hump was redder than that at the bottom of the superhumps, as indicated by the dashed line in the figure. The reddest phase (~ 0.7) significantly preceded the bottom of the superhump (~ 0.0).

It is noteworthy that the primary and secondary humps exhibited different behaviors in $V - J$. In the “blue” primary hump, the observed feature can be explained by heating and subsequent cooling processes at the outermost

part of the accretion disk. In superhumps, the heating mechanism is tidal dissipation (Osaki 1996). The precedence of the bluest phase suggests that the heating process finished before the superhump maximum. Then, the object reached the superhump maximum by an expansion of the low temperature region in the accretion disk. In the “red” secondary hump, the latter effect, namely, the expansion of a low temperature region, is probably more substantial.

4. Discussion

As shown in the last section, J0557+68 has a relatively short T_s (480 d) and a quite short P_{orb} . T_s is much shorter than those of WZ Sge stars which are a dominant population in the shortest P_{orb} regime. The characteristics of J0557+68 are reminiscent of V844 Her (Thorstensen et al. 2002b). As well as J0557+68 and V844 Her, recent studies have shown several objects in the shortest P_{orb} regime having observational features distinct from those of WZ Sge stars, such as PU CMA (Kato et al. 2003b) and LL And (Kato 2004). On the other hand, there is no established classification of DNe in the shortest P_{orb} regime that includes the above anomalies. In order to study the nature of J0557+68, it is important to identify its possible companions and search their common features. In this section, we present a new exploratory classification of DNe in the shortest P_{orb} regime using hierarchical cluster analysis. We discuss not only the nature of J0557+68, but also the origin of the observed diversity in T_s based on the identified clusters.

4.1. Classification of DNe in the shortest P_{orb} regime by hierarchical cluster analysis

We list SU UMa-type DNe having short P_{orb} (< 95 min) in table 5. The table shows T_s , outburst amplitude Δm , and superhump period excess $\varepsilon \equiv (P_{\text{SH}} - P_{\text{orb}})/P_{\text{orb}}$. The table only includes confirmed SU UMa stars in which superhumps were observed during past superoutbursts. The objects and their parameters in the table were generally quoted from the Ritter & Kolb catalog ver. 7.9 (RKcat7.9; Ritter, Kolb 2003). Some of the parameters were updated by the references and recent superoutbursts shown in the table. The dates of the recent superoutbursts were referred from the VSNET and ASAS-3 database (Kato et al. 2004b; Pojmanski 2002).

According to the disk instability model, T_s and ε can be indicators of the mass-transfer rate and the mass ratio of the binary, respectively (Osaki 1996; Patterson et al. 2005a). Δm has historically been considered to be a key parameter for dividing DNe into WZ Sge and normal SU UMa systems (Howell et al. 1995; Kato et al. 2001b).

The parameters are plotted against P_{orb} in figure 9. J0557+68 is indicated by the large open circle with its P_{SH} . The anomalous feature of J0557+68 is evident: short T_s and small Δm , compared with the other short P_{orb} systems having $76 \text{ min} \lesssim P_{\text{orb}} \lesssim 85 \text{ min}$. According to the disk instability theory, the short T_s suggests that the mass-transfer rate of J0557+68 is exceptionally high compared

with the systems having similar short P_{orb} .

Hierarchical cluster analysis was performed using the four parameters P_{orb} , $\log(T_s)$, Δm , and ε . As the parameters have different dimensions, for the cluster analysis the observed values were transformed to so-called “Z-scores” defined as $(a - \bar{a})/\sigma_a$, where a , \bar{a} , and σ_a are the parameter value, its average, and standard deviation, respectively. The sample consists of 34 objects selected from table 5 in which all four parameters are known. HO Del and AQ CMi were not included in the sample because their T_s is uncertain.

The calculation was performed with the `pvclust`² package of R³. Using the `pvclust` function, we can estimate the confidence level (or probability value; p -value) for clusters via the multi-scale bootstrap re-sampling method (Shimodaira 2004). The bootstrap samples were generated by randomly drawing N samples with replacement from the original sample, where N is the number of samples. The p -value was approximated as the probability that the cluster is obtained in the bootstrap replicates of the dendrogram, shown in percentage. A high value indicates a high significance. In this paper, we only discuss clusters having $p \geq 95$ %. For the dendrogram classification method, we used Ward’s method in which the within-class variance is minimized and the between-class variance is maximized (Murtagh, Heck 1987). This method is commonly used for cases where the number of samples is small. It has the advantage of being able to derive small independent clusters, avoiding the need to form large chain-shaped clusters containing small clusters (Milligan 1980). Since our sample size is small, it is suitable for our analysis.

The obtained dendrogram is depicted in figure 10. We identified six clusters which have p -values higher than 95 with a singleton cluster of DI UMa. The errors of the p -values were estimated to be less than 1 % in the range of $p \geq 95$ %. The seven clusters are labeled “SU”, “DI”, “ER”, “WZ”, “V485”, “SU/WZ”, and “X” in the figure. The average parameters for each cluster are shown in figure 11 as filled circles. We describe the characteristics of each cluster as follows:

- *Group SU* consists of normal SU UMa stars. The minimum P_{orb} is 86 min in this group. We consider that most SU UMa stars having $P_{\text{orb}} > 95$ min also have the same nature as this group.
- *Group WZ* includes so-called WZ Sge stars. This group is characterized by short P_{orb} , long T_s , large Δm , and small ε , as can be seen in figure 11.
- *Group SU/WZ* is located between *Group SU* and *Group WZ* in all parameter spaces, as shown in figure 11. All the systems in this group are listed as “large-amplitude SU UMa-type DNe” in Kato et al. (2001b), except for HV Vir. HV Vir has been considered as a WZ Sge star since it exhibited early superhumps which are only seen in that group (Kato et al. 2001b). However, HV Vir is not classified into

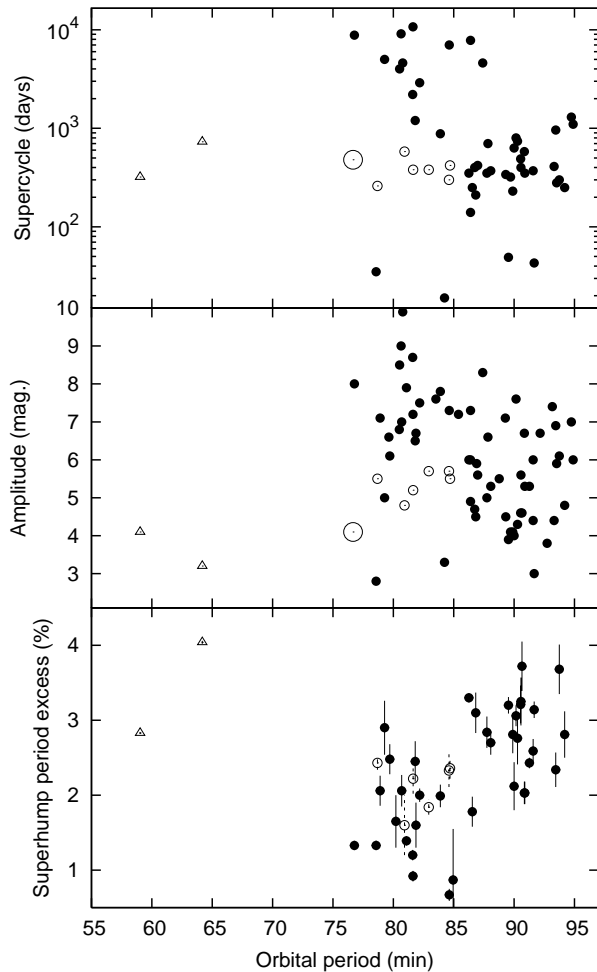


Fig. 9. Supercycle, outburst amplitude, and superhump period excess of short period SU UMa-type DNe ($P_{\text{orb}} < 95$ min) as a function of the orbital period. The open circles indicate systems categorized in a group having short P_{orb} and short supercycles. The large open circles denote J0557+68 with P_{SH} . The open triangles indicate V485 Cen and EI Psc. The filled circles indicate the other systems.

Group WZ, but rather into *SU/WZ* in our cluster analysis because of its relatively short T_s and large ε compared with those in *Group WZ*. BC UMa is also a noteworthy member of this group. Maehara et al. (2007) reported the detection of early superhumps in this object, while BC UMa has an atypically long P_{orb} for WZ Sge stars. They propose that BC UMa has an intermediate nature between normal SU UMa and WZ Sge stars. *Group SU/WZ* may be considered as an intermediate evolutionary stage between *Group SU* and *WZ*.

- *Group V485* contains two peculiar systems, V485 Cen and EI Psc. They are indicated by open triangles in figure 9. As described in § 1, they have evolved secondaries and hence are proposed to be on a different evolutionary path from those of CVs having main-sequence secondaries (Augusteyn et al.

² <http://www.is.titech.ac.jp/~shimo/prog/pvclust/>

³ <http://www.R-project.org>

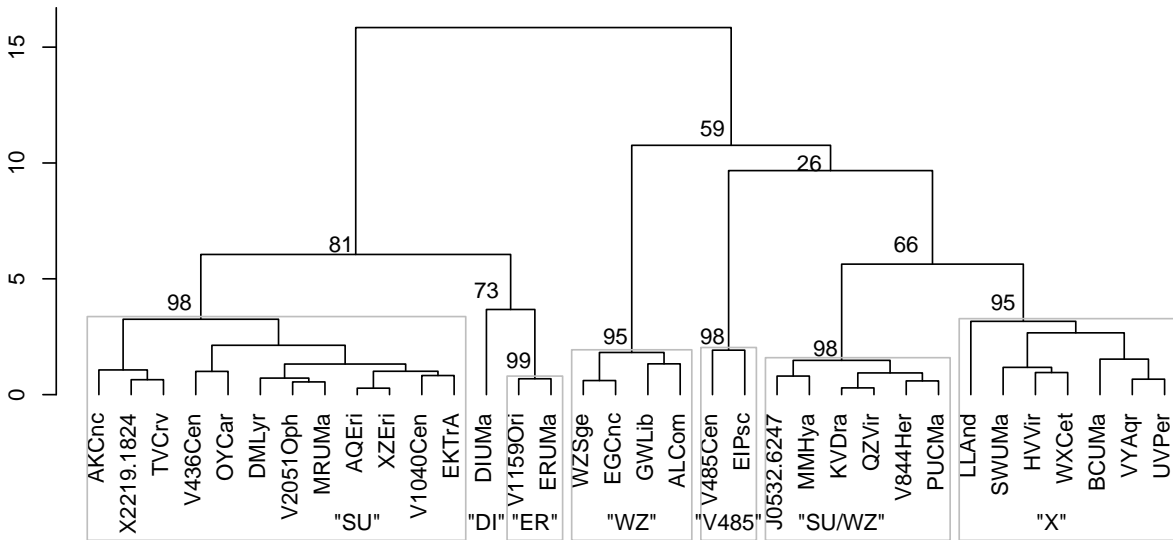


Fig. 10. Cluster dendrogram of short- P_{orb} DNe. The vertical axis is a measure of the Euclidean dissimilarity. Shown are p -values for the clusters calculated with the multi-scale bootstrap re-sampling method (Shimodaira 2004).

- 1996; Thorstensen et al. 2002a; Uemura et al. 2002).
- *Group ER* is so-called “ER UMa stars”, which are characterized by quite short T_s (Kato, Kunjaya 1995). In addition to ER UMa and V1159 Ori, IX Dra is also considered to be in this group (Ishioka et al. 2001a).
 - *Group DI* is a singleton cluster of DI UMa. In general, this object is considered as a member of, so-called, “ER UMa stars”. Our cluster analysis divided ER UMa stars into *Group ER* and *DI*, probably because of a very short P_{orb} of DI UMa compared with those of ER UMa and V1159 Ori.
 - *Group X* is a group established by our analysis for the first time. The members of this group are indicated by small open circles in figure 9. They have quite short P_{orb} , although T_s is about one order of magnitude shorter than those of “WZ” on average, as can be seen in figure 11. Δm is also much smaller than those of “WZ” and “SU/WZ”. ε is significantly larger than those of “WZ”.

Our classification method adequately reproduced the previously known sub-groups. In addition, we identified a new noteworthy group, *Group X*, which may be a key group for the study of CV evolution.

4.2. On the nature of J0557+68 and *Group X*

J0557+68 presumably belongs to *Group X* because of the short T_s and small Δm . The result of the cluster analysis therefore predicts that J0557+68 has a relatively large ε compared with those of WZ Sge stars. Using the average value of ε in *Group X* ($\varepsilon = 2.2 \pm 0.3$), the P_{orb} of J0557+68 is calculated to be 0.05209 ± 0.00015 d.

According to Podsiadlowski et al. (2003), CVs with

evolved secondaries can have P_{min} shorter than that of CVs having main-sequence secondaries. Such objects have high mass-transfer rates before evolving to longer periods compared with ordinary CVs, and finally evolve to AM CVn stars after passing P_{min} . V485 Cen and EI Psc may be objects on this evolutionary channel (Uemura et al. 2002). As well as V485 Cen and EI Psc, objects on that evolutionary channel are expected to be found in the CV population with $P_{\text{orb}} > 76$ min. Such progenitors of AM CVn and V485 Cen-like objects definitely have a comparable or higher mass-transfer rate compared with V485 Cen-like objects. As a result, they should have comparable or shorter T_s than those of ordinary objects. This might cause the observed diversity in T_s in the shortest P_{orb} regime (Thorstensen et al. 2002b). Possible candidates for such anomalies are ER UMa stars and objects in *Group X*.

The mass-transfer rate in ER UMa stars should be one order higher than those of normal SU UMa stars in order to reproduce the quite short T_s (Kato, Kunjaya 1995; Osaki 1995a). If ER UMa stars are a progenitor of V485 Cen-like objects, the mass-transfer rate must rapidly decrease by one order of magnitude from $P_{\text{orb}} \sim 90$ min to ~ 60 min. The evolutionary path calculated by Podsiadlowski et al. (2003), however, shows a rather gradual decrease of the mass-transfer rate before P_{min} . The small ε of DI UMa, furthermore, indicates a small mass of the secondary. Thorstensen et al. (2002b) reported that the optical spectrum of DI UMa is typical for ordinary DNe at quiescence with none of the TiO absorption bands observed in V485 Cen and EI Psc. These observations are unfavorable for the scenario that ER UMa stars have evolved secondaries and are progenitors of V485 Cen-like

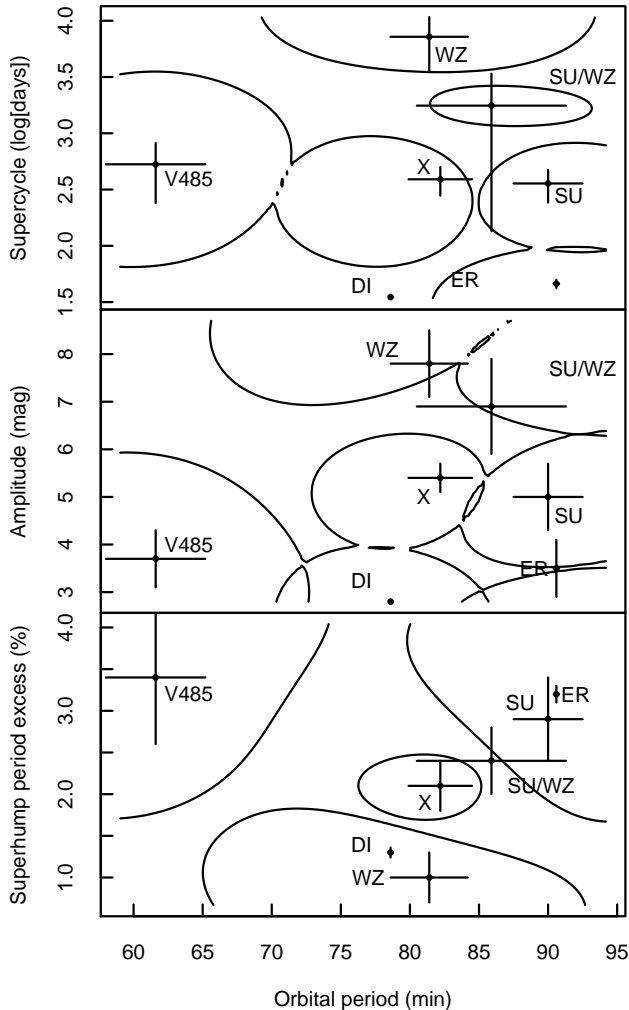


Fig. 11. As for figure 9, but for the averages of the parameters in sub-groups defined by our cluster analysis (for detail, see the text). The filled circles and error bars indicate the averages and standard deviations, respectively. The solid curves indicate the decision boundaries for each category, calculated by the support vector machine (SVM) method.

objects.

No evidence of evolved secondaries is seen either in the objects of *Group X*. The average ε of the objects in *Group X* are smaller than those in *Group V485*, as can be seen in the bottom panel of figure 11. This implies that the objects in *Group X* have a secondary mass smaller than those of V485 Cen-like objects (Patterson et al. 2005a). Thorstensen et al. (2002b) reported that the optical spectrum of V844 Her, a member of *Group X*, is also typical for ordinary DNe at quiescence.

We noticed a peculiar outburst activity, observed in several objects in *Group X*. It is known that V844 Her experiences only a few normal outbursts and that most of the outbursts are superoutbursts (Kato, Uemura 2000; Oizumi et al. 2007). The disk instability model predicts that a system with a higher mass-transfer rate experiences more frequent normal outbursts (Osaki 1996). ER UMA

stars actually show frequent normal outbursts, as predicted. If V844 Her has an evolved secondary, the mass-transfer rate is expected to be high. However, the scarcity of normal outbursts appears to contradict disk instability theory. QZ Vir, a member of *Group X*, also exhibits few normal outbursts. Since QZ Vir is a bright source, it is less likely that a significant number of normal outbursts have been overlooked. In addition, no normal outbursts have been reported for J0557+68 based on the VSNET database (Kato et al. 2004b).

The scarcity of normal outbursts in those systems is reminiscent of WZ Sge stars having a low mass-transfer rate. According to disk instability theory, the mass-transfer rate in WZ Sge stars is so low that the recurrence time of normal outbursts exceeds T_s (Osaki 1995b). As a result, WZ Sge stars only show superoutbursts. It is possible that the objects in *Group X* have low mass-transfer rates, like WZ Sge stars, while superoutbursts are frequently triggered due to an atypically high viscosity in the quiescent accretion disk. In this case, the observed diversity in T_s in the shortest P_{orb} regime is not due to the diversity in the evolutionary path of objects, but due to the diversity in accretion-disk structures.

The nature of *Group X* is still an open issue. Imada et al. (2006a) propose that the short P_{orb} DN SDSS J013701.06–091234.9 has a luminous and evolved secondary since it shows significant TiO absorption and red infrared colors. As shown in table 5, the Δm and ε of SDSS J013701.06–091234.9 suggest that it is a possible member of *Group X*. This implies that a small portion of DNe having $P_{\text{orb}} \gtrsim 76$ min have evolved secondaries and hence are progenitors of AM CVn or V485 Cen-like objects. Dynamical estimations of the secondary mass with radial velocity studies are required for DNe in the shortest P_{orb} regime in order to explore the origin of the diversity in T_s . Our cluster analysis provides high-priority objects for future studies, that is, members of *Group X*.

4.3. Estimation of boundaries of groups with the support vector machine method

The above seven groups of DNe were defined in four-parameter space. Now we estimate the boundaries of the groups in two-parameter spaces, that is, P_{orb} and the other three parameters. This is useful for categorizing objects if only some of the parameters are known.

The support vector machine (SVM) method provides a means to estimate the optimal decision boundaries of the groups (Vapnik 1998; Chen et al. 2005). The SVM constructs a linear classification between two groups by defining an optimal hyperplane which separates members of the groups. The optimal plane is determined by maximizing the margin between the opposing group members closest to the plane. The original SVM can be extended for non-linear classifications by using kernels to project the data into a higher dimensional space (Boser et al. 1992). An improved SVM called the soft margin SVM can tolerate minor misclassifications (Cortes and Vapnik 1995). In this paper, we used a soft-margin SVM with a radial-based kernel.

We estimated the boundaries of a group against the other groups using the result of the cluster analysis. The calculations were performed by the `svm` function (C-classification) in the `e1071` package of `R`. The width of an allowable margin around the separating plane is defined by a parameter “*C*”. We determined the parameter “*C*” by maximizing the region of the groups and minimizing the overlapped areas between the regions. The calculated boundaries are indicated by solid curves in figure 11. As can be seen in figure 11, the boundaries fail to identify several groups: no boundary is given for *Group ER* and *SU/WZ* in the ε - P_{orb} plane, and the boundary of *Group DI* is given only for Δm - P_{orb} plane. This is because the number of the sample is small and the members of these groups are blended in the other group members in the ε - P_{orb} plane.

In table 5, we show the group identification in parentheses, for example “(SU)”, for objects which were not used for the cluster analysis. These objects were classified following the boundaries estimated by SVM. In addition, objects were labeled “(WZ)” when i) early superhumps were detected and ii) the system experienced the rebrightening phenomenon which characterizes WZ Sge-type superoutbursts (Kato et al. 2004a). *Group SU*, *SU/WZ*, and *WZ* and their possible members account for 70% and 95% of DNe with $P_{\text{orb}} < 86$ min and $86 \text{ min} \leq P_{\text{orb}} < 95$ min, respectively. Thus, we have confirmed that these three groups are the major population in those P_{orb} regimes.

5. Summary

We observed J0557+68 during the outburst in December 2006. Our observation revealed that the object is an SU UMa-type DN having a quite short superhump period of $P_{\text{SH}} = 0.05324 \pm 0.00002$ d. The next superoutburst occurred in March 2008. The T_s of this object is, hence, estimated to be 480 d, which is much shorter than those of WZ Sge stars. Using the cluster analysis, we found that a peculiar group characterized by short T_s has P_{orb} slightly longer than P_{min} . J0557+68 probably belongs to this group. While the nature of this group is still an open issue, its peculiar feature of a short T_s is possibly due to an atypically high viscosity in quiescent disks or due to the evolutionary sequence being different from ordinary CVs having main-sequence secondaries.

This work was partly supported by a Grand-in-Aid from the Ministry of Education, Culture, Sports, Science, and Technology of Japan (17684004, 17340054, 18740153, 14079206, 18840032, 19740104).

References

Arai, A., Uemura, M., Sasada, M., Schmeer, P., & Miller, I. 2009, in ASP Conf. Ser. , The 8th Pacific Rim Conference on Stellar Astrophysics, ed. B. Soonthornthum, S. Komonjinda, K. S. Cheng, & K. Leung (San Francisco: ASP), in press.
 Augusteijn, T., van der Hooft, F., de Jong, J. A., & van Paradijs, J. 1996, A&A, 311, 889

Baba, H., Kato, T., Nogami, D., Hirata, R., Matsumoto, K., & Sadakane, K. 2000, PASJ, 52, 429
 Boser, B. E., Guyon, I. M., & Vapnik, V. N. 1992, in Proceedings of the fifth annual workshop on COLT, ed. D. Haussler, (Pittsburgh: ACM Press), 144
 Chen, P. H., Lin, C. J., & Scholkopf, B. 2005, Appl. Stoch. Models Bus. Ind., 21, 111
 Cortes, C. & Vapnik, V. 1995, Machine Learning, 20, 273
 Gilks, W. R., Richardson, S., & Spiegelhalter, D. J., 1996, Markov chain Monte Carlo in practice (Chapman & Hall)
 Howell, S. B., Szkody, P., & Cannizzo, J. K. 1995, ApJ, 439, 337
 Imada, A. 2008, PhD thesis, Department of Astronomy, Faculty of Science, Kyoto University, Kitashirakawa-Oiwake-cho, Sakyo-ku, Kyoto 606-8502, Japan
 Imada, A. & Monard, L. A. G. B. 2006, PASJ, 58, L19
 Imada, A., Kato, T., Kubota, K., Uemura, M., Ishioka, R., Kiyota, S., Kinugasa, K., Maehara, H., et al. 2006a, PASJ, 58, 143
 Imada, A., Kubota, K., Kato, T., Nogami, D., Maehara, H., Nakajima, K., Uemura, M., & Ishioka, R. 2006b, PASJ, 58, L23
 Ishioka, R., Kato, T., Uemura, M., Iwamatsu, H., Matsumoto, K., Martin, B. E., Billings, G. W., & Novak, R. 2001a, PASJ, 53, L51
 Ishioka, R., Kato, T., Uemura, M., Iwamatsu, H., Matsumoto, K., Stubbings, R., Mennickent, R., Billings, G. W., et al. 2001b, PASJ, 53, 905
 Kapusta, A. B. & Thorstensen, J. R. 2006, PASP, 118, 1119
 Kato, T. & Kunjaya, C. 1995, PASJ, 47, 163
 Kato, T., Nogami, D., & Baba, H. 1995, IBVS, 4228
 Kato, T., Nogami, D., Baba, H., Matsumoto, K., Arimoto, J., Tanabe, K., & Ishikawa, K. 1996, PASJ, 48, L21
 Kato, T., Matsumoto, K., & Stubbings, R. 1999, IBVS, 4760
 Kato, T. & Uemura, M. 2000, IBVS, 4902
 Kato, T., Nogami, D., Lockley, J. J., & Somers, M. 2001a, IBVS, 5116
 Kato, T., Sekine, Y., & Hirata, R. 2001b, PASJ, 53, 1191
 Kato, T., Nogami, D., Moilanen, M., & Yamaoka, H. 2003a, PASJ, 55, 989
 Kato, T., Santallo, S., Bolt, G., Richards, T., Nelson, P., Monard, B., Uemura, M., Kiyota, S., et al. 2003b, MNRAS, 339, 861
 Kato, T. 2004, PASJ, 56, 135
 Kato, T., Nogami, D., Matsumoto, K., & Baba, H. 2004a, PASJ, 56, 109
 Kato, T., Uemura, M., Ishioka, R., Nogami, D., Kunjaya, C., Baba, H., & Yamaoka, H. 2004b, PASJ, 56, 1
 Kato, T., Imada, A., Uemura, M., Nogami, D., Maehara, H., Ishioka, R., Baba, H., Matsumoto, K., et al. 2009, PASJ, in press. (eprint arXiv:0905.1757)
 Kloehr, W., Torii, K., Maehara, H., Trontal, O., & Boyd, D. 2006, Central Bureau Electronic Telegrams, 777, 1
 Koen, C. 2006, MNRAS, 365, 489
 Kolb, U. 1993, A&A, 271, 149
 Kolb, U. & Baraffe, I. 1999, MNRAS, 309, 1034
 Kurochkin, N. E. 1984, Astron. Tsirk., 1325, 5
 Leibowitz, E. M., Mendelson, H., Bruch, A., Duerbeck, H. W., Seitter, W. C., & Richter, G. A. 1994, ApJ, 421, 771
 Maehara, H., Hachisu, I., & Nakajima, K. 2007, PASJ, 59, 227
 Milligan, N. 1953, The journal of chemical physics, 21, 1087
 Milligan, G. W. 1980, Psychometrika, 45, 1860
 Murtagh, F. & Heck, A. 1987, Multivariate Data Analysis (Reidel: Dordrecht)

- Novák, R., Vanmunster, T., Jensen, L. T., & Nogami, D. 2001, *IBVS*, 5108
- Oizumi, S., Omodaka, T., Yamamoto, H., Tanada, S., Yasuda, T., Arai, Y., Kodama, K., Suzuki, M., et al. 2007, *PASJ*, 59, 643
- Olech, A. 1997, *Acta Astron.*, 47, 281
- Osaki, Y. 1995a, *PASJ*, 47, L11
- Osaki, Y. 1995b, *PASJ*, 47, 47
- Osaki, Y. 1996, *PASP*, 108, 39
- Paczynski, B. 1981, *Acta Astronomica*, 31, 1
- Patterson, J., Kemp, J., Harvey, D. A., Fried, R. E., Rea, R., Monard, B., Cook, L. M., Skillman, D. R., et al. 2005a, *PASP*, 117, 1204
- Patterson, J., Thorstensen, J. R., Armstrong, E., Henden, A. A., & Hynes, R. I. 2005b, *PASP*, 117, 922
- Pavlenko, E., Shugarov, S. Y., Katysheva, N. A., Nogami, D., Nakajima, K., Maehara, H., Andreev, M., Shimansky, V., et al. 2007, in *ASP Conf. Ser. 372*, European Workshop on White Dwarfs, ed. R. Napiwotzki, & M. R. Burleigh (San Francisco: ASP), 511
- Pavlov, M. V. & Shugarov, S. Y. 1985, *Astron. Tsirk.*, 1373, 8
- Perryman, M. A. C. & ESA 1997, *The HIPPARCOS and TYCHO catalogues. Astrometric and photometric star catalogues derived from the ESA HIPPARCOS Space Astrometry Mission Vol. 1200 of ESA Special Publication*
- Podsiadlowski, P., Han, Z., & Rappaport, S. 2003, *MNRAS*, 340, 1214
- Pojmanski, G. 2002, *Acta Astron.*, 52, 397
- Price, A., Gary, B., Bedient, J., Cook, L., Templeton, M., Pullen, C., Starkey, D., Crawford, T., et al. 2004, *PASP*, 116, 1117
- Rappaport, S., Joss, P. C., & Webbink, R. F. 1982, *ApJ*, 254, 616
- Renoizé, V., Baraffe, I., Kolb, U., & Ritter, H. 2002, *A&A*, 389, 485
- Renz, W., Hanisch, J., Lindberg, H.-G., Boyd, D., Waagen, E., Quinn, N., Rodriguez, D., McGaha, J. E., et al. 2005, *IAU Circ.*, 8591, 2
- Ritter, H. & Kolb, U. 2003, *A&A*, 404, 301
- Rodriguez-Gil, P., Gänsicke, B. T., Hagen, H.-J., Marsh, T. R., Harlaftis, E. T., Kitsionas, S., & Engels, D. 2005, *A&A*, 431, 269
- Shafter, A. W., Coelho, E. A., & Reed, J. K. 2007, *PASP*, 119, 388
- Shears, J. 2009, *Journal of Am. Assoc. Var. Star. Soc.*, 37, 1
- Shears, J., Boyd, D., Krajci, T., Koff, R., Thorstensen, J. R., & Poyner, G. 2008a, *Journal of the British Astronomical Association*, 118, 95
- Shears, J., Brady, S., Foote, J., Starkey, D., & Vanmunster, T. 2008b, *Journal of the British Astronomical Association*, 118, 288
- Shimodaira, H. 2004, *Annals of Statistics*, 32, 2616
- Skrutskie, M. F., Cutri, R. M., Stiening, R., Weinberg, M. D., Schneider, S., Carpenter, J. M., Beichman, C., Capps, R., et al. 2006, *AJ*, 131, 1163
- Stellingwerf, R. F. 1978, *ApJ*, 224, 953
- Sterken, C., Vogt, N., Schreiber, M. R., Uemura, M., & Tuvikene, T. 2007, *A&A*, 463, 1053
- Templeton, M. R., Leaman, R., Szkody, P., Henden, A., Cook, L., Starkey, D., Oksanen, A., Koppelman, M., et al. 2006, *PASP*, 118, 236
- Thorstensen, J. R., Fenton, W. H., Patterson, J. O., Kemp, J., Krajci, T., & Baraffe, I. 2002a, *ApJL*, 567, L49
- Thorstensen, J. R., Patterson, J. O., Kemp, J., & Vennes, S. 2002b, *PASP*, 114, 1108
- Uemura, M. & Arai, A. 2006, *Central Bureau Electronic Telegrams*, 777, 2
- Uemura, M., Kato, T., Ishioka, R., Yamaoka, H., Schmeer, P., Starkey, D. R., Torii, K., Kawai, N., et al. 2002, *PASJ*, 54, 599
- Uemura, M., Kato, T., Ishioka, R., Bolt, G., Cook, L. M., Monard, B., Stubbings, R., Torii, K., et al. 2003, *PASJ*, 56, S141
- Uemura, M., Mennickent, R. E., Ishioka, R., Imada, A., Kato, T., Nogami, D., Stubbings, R., Kiyota, S., et al. 2005, *A&A*, 432, 261
- Uemura, M., Arai, A., Krajci, T., Pavlenko, E., Shugarov, S. Y., Katysheva, N. A., Goranskij, V. P., Maehara, H., et al. 2008, *PASJ*, 60, 227
- Vanmunster, T., Krajci, T., Monard, B., Cook, L. M., de Ponthiere, P., Boyd, D., Crawford, T. R., Armstrong, M. J., & Rodriguez, D. 2006, *Society for Astronomical Sciences Annual Symposium*, 25, 77
- Vapnik, V. N. 1998, *Statistical Learning Theory* (New York:Wiley)
- Warner, B. 1995a, *Cataclysmic Variable Stars* (Cambridge University Press)
- Warner, B. 1995b, *Ap&SS*, 226, 187
- Watanabe, M., Nakaya, H., Yamamuro, T., Zenno, T., Ishii, M., Okada, M., Yamazaki, A., Yamanaka, Y., et al. 2005, *PASP*, 117, 870

Table 5. Parameters of DNe having a short period of $P_{\text{orb}} \leq 95$ min.

P_{orb} (min)	T_s (d)	Δm (mag)	ε (%)	Object	Group	Outburst dates
59.0328	320	4.1 ¹	2.83 ± 0.01^2	V485 Cen	V485	
64.1765	730	3.2	4.04 ± 0.02^3	EI Psc	V485	2005.08, 2007.08
—	480	4.1	—	J0557+6832	(X)	2006.12, 2008.03
76.0320	—	>5.8	—	J0329+1250	(WZ?)(X?) ⁴	2006.10
76.7808	8800	8.0	1.33 ± 0.04^5	GW Lib	WZ	1983.08 ⁶ , 2007.04
78.5722	35	2.8 ¹	1.33 ± 0.06^5	DI UMa	DI	
78.6859	260 ⁷	5.5 ¹	2.43 ± 0.09^5	V844 Her	X	
78.9120	—	>4.6 ¹	—	J0222+4122	(WZ) ⁸	2005.11
78.9120	—	7.1	2.06 ± 0.20^9	J0233–1047	(WZ) ⁹	2006.01
79.2792	5000 ⁷	5.0	2.90 ± 0.36	LL And	X	
79.6320	—	6.6 ¹	—	V2176 Cyg	(WZ)	1997.08 ¹⁰
79.7054	—	6.1	2.48 ± 0.20^5	J0137–0912	(X)	2003.12
80.2080	—	>5.5	1.65 ± 0.35^{11}	SS LMi	(WZ?)	2006.10
80.4960	—	6.8 ¹²	—	J1021+2349	(WZ) ¹²	2006.11
80.5248	$\sim 4000^7$	8.5	—	V592 Her	(WZ)	
80.6400	$\sim 9100^{13}$	9.0	—	PQ And	(WZ)	
80.6976	—	7.0	2.06 ± 0.21^5	J0025+1217	(WZ) ¹⁴	2004.09
80.7840	4600	9.9	—	UW Tri	(WZ)	1983.09 ¹⁵ , 1995.03 ¹⁶ , 2008.10
80.9280	580	4.8 ¹	1.60 ± 0.40^{17}	J0532+6247	X	2006.06, 2008.01
81.0850	—	7.9	1.39 ± 0.02	V455 And	(WZ)	2007.09
81.6019	2200	8.7	1.20 ± 0.07^5	AL Com	WZ	1995.04 ¹⁸ , 2001.05, 2007.11
81.6307	10700 ⁷	7.2	0.92 ± 0.07^5	WZ Sge	WZ	
81.6394	380 ⁷	5.2	2.22 ± 0.20^5	PU CMa	X	
81.8136	1200	6.5 ⁵	2.45 ± 0.27^7	SW UMa	SU/WZ	2000.02, 2002.10, 2006.09
81.8784	—	6.7	1.60 ± 0.30^{19}	V1108 Her	(WZ) ¹⁹	2004.06
82.1794	2900	7.5	2.00 ± 0.09^5	HV Vir	(WZ)	1992.04 ²⁰ , 2002.01, 2008.01
82.9296	380 ⁷	5.7	1.84 ± 0.10^5	MM Hya	X	
83.5200	—	7.6	—	J1959+2242	(WZ) ²¹	2005.08
83.8958	880 ²²	7.8 ¹	1.99 ± 0.15^5	WX Cet	SU/WZ	
84.0960	—	>7.1	—	J1112–3538	(WZ) ²³	2007.12
84.2400	19	3.3 ¹	—	RZ LMi	(ER?)(DI?)	
84.6144	300 ²⁴	5.7 ¹	2.33 ± 0.22^5	KV Dra	X	
84.6288	7000 ⁷	7.3	0.67 ± 0.08^5	EG Cnc	WZ	
84.7008	420 ⁷	5.5 ¹	2.36 ± 0.14^5	QZ Vir	X	
84.7584	—	>5.8 ¹	—	FL TrA	(SU)	2005.07
84.9600	—	>5.2	0.87 ± 0.68^{25}	J0804+5103	(WZ)	2006.03
85.3920	—	7.2	—	V585 Lyr	(SU/WZ)	2003.09
86.2560	350	6.0	3.30 ± 0.01^{26}	2219+1824	SU	
86.4000	—	7.3	—	J0807+1138	(SU/WZ)	2007.11
86.4000	140 ⁷	4.9 ¹	—	CI UMa	(SU)	
86.4000	7800	6.0	—	DV Dra	(WZ)	1984.06 ²⁷ , 2005.11
86.5440	250	>5.0	1.78 ± 0.20^5	RX Vol	(SU)	2006.10, 2007.06, 2008.02
86.7456	400 ⁷	4.7 ¹	—	MM Sco	(SU)	
86.8320	210 ⁷	4.5 ¹	3.10 ± 0.27^5	V1040 Cen	SU	
86.9040	—	5.9	—	KX Aql	(SU)	1980.11 ²⁸
86.9904	420 ⁷	5.6 ¹	—	V1028 Cyg	(SU)	
87.4080	4600	8.3	—	UZ Boo	(WZ)	1978.09 ²⁸ , 1994.08 ²⁸ , 2003.12
87.7536	350	5.0	2.84 ± 0.21^5	AQ Eri	SU	2006.11, 2007.12, 2008.12
87.8400	700	6.6	—	V1454 Cyg	(SU)	2004.12, 2006.11
88.0690	370	5.3	2.70 ± 0.16^5	XZ Eri	SU	2007.12, 2008.11 ²⁹
88.7760	—	5.5	—	J0918–2942	(SU)	
89.2800	—	7.1	—	J1025–1542	(WZ) ⁷	2006.02
89.3088	340 ⁷	4.5 ¹	—	V1141 Aql	(SU)	
89.5363	49	3.9 ¹	3.20 ± 0.11^5	V1159 Ori	ER	

Table 5. (Continued.)

P_{orb} (min)	T_s (d)	Δm (mag)	ε (%)	Object	Group	Outburst dates
89.7120	—	>8.3	—	CG CMa	(WZ) ³⁰	1991 ³⁰
89.7120	320	4.1 ¹	—	V402 And	(SU)	2005.10, 2006.08, 2007.07
89.8963	230 ⁷	4.1 ¹	2.81 ± 0.25^5	V2051 Oph	SU	
90.0014	630 ⁷	4.0	2.12 ± 0.32^5	V436 Cen	SU	
90.1584	800 ³¹	7.6	3.06 ± 0.14^5	BC UMa	SU/WZ	
90.2880	$\sim 740^6$	4.3	2.76 ± 0.35^5	HO Del	(SU)	
90.5472	490 ⁷	4.6	3.21 ± 0.25^5	EK TrA	SU	
90.5760	400 ³²	5.6	3.25 ± 0.32^5	TV Crv	SU	
90.6624	—	4.6	3.72 ± 0.33^{33}	J1227+5139	(SU)	2007.06
90.8496	580 ⁷	6.7	2.03 ± 0.15^5	VY Aqr	SU/WZ	
90.8942	350 ⁷	5.3	2.03 ± 0.15^5	OY Car	SU	
91.2672	—	5.3	2.43 ± 0.07^{34}	J1600–4846	(SU)	2005.06
91.5840	—	6.0	—	J1536–0839	(SU)	2004.02
91.5840	370 ⁷	4.4	2.59 ± 0.16^5	MR UMa	SU	
91.6704	43 ¹	3.0	3.14 ± 0.11^5	ER UMa	ER	
92.1600	—	6.7	—	DO Vul	(SU)	2005.11
92.7360	—	3.8 ¹	—	J1653+2010	(SU)	2004
93.1680	—	7.4	—	J0232–3717	(WZ) ³⁵	2007.09
93.3120	$\sim 410^6$	4.4	—	AQ CMi	(SU)	
93.4560	960 ⁷	6.9	2.34 ± 0.23^5	UV Per	SU/WZ	
93.5280	280 ⁷	5.9	—	CT Hya	(SU)	
93.7440	300 ⁷	6.1	3.68 ± 0.33^5	AK Cnc	SU	
94.1890	250 ⁷	4.8	2.81 ± 0.31^5	DM Lyr	SU	
94.7520	1300	7.0	—	GO Com	(SU)	1995.07 ³⁶ , 2003.06, 2006.12
94.8960	1100	6.0	—	V551 Sgr	(SU)	2003.09, 2006.08

The parameters are quoted from Ritter, Kolb (2003) or references below. 1. Imada (2008), 2. Olech (1997), 3. Uemura et al. (2002), 4. Shafter et al. (2007), 5. Patterson et al. (2005a), 6. Gonzalez 1983, 7. Kato et al. (2003a), 8. Imada et al. (2006b), 9. Vanmunster et al. (2006), 10. Novák et al. (2001), 11. Shears et al. (2008a), 12. Uemura et al. (2008), 13. Patterson et al. (2005b), 14. Templeton et al. (2006), 15. Kurochkin (1984), 16. Kato et al. (2001a), 17. Kapusta, Thorstensen (2006), 18. Kato et al. (1996), 19. Price et al. (2004), 20. Leibowitz et al. (1994), 21. Renz et al. (2005), 22. Sterken et al. (2007), 23. Maehara (2007)⁴, 24. Shears (2009), 25. Pavlenko et al. (2007), 26. Rodríguez-Gil et al. (2005), 27. Pavlov, Shugarov (1985), 28. Kato et al. (2001b), 29. Uemura et al. (2004), 30. Kato et al. (1999), 31. Maehara et al. (2007), 32. Uemura et al. (2005), 33. Shears et al. (2008b), 34. Imada, Monard (2006), 35. Arai et al. (2009), 36. Kato et al. (1995)